Uniaxial Compression Behavior of Bulk Nano-twinned Gold from Molecular Dynamics Simulation

Chuang Deng, and Frederic Sansoz
School of Engineering, University of Vermont, Burlington, VT, 05482

ABSTRACT

Parallel molecular dynamics simulations were used to study the influence of pre-existing growth twin boundaries on the slip activity of bulk gold under uniaxial compression. The simulations were performed on a 3D, fully periodic simulation box at 300 K with a constant strain rate of 4×10^7 s^{-1}. Different twin boundary interspacings from 2 nm to 16 nm were investigated. The strength of bulk nano-twinned gold was found to increase as the twin interspacing was decreased. However, strengthening effects related to the twin size were less significant in bulk gold than in gold nanopillars. The atomic analysis of deformation modes at the twin boundary/slip intersection suggested that the mechanisms of interfacial plasticity in nano-twinned gold were different between bulk and nanopillar geometries.

INTRODUCTION

The uniaxial deformation of micro/nano-sized gold pillars by nanoindentation has provided new fundamental insights into the influence of sample size on plasticity and strengthening in metals [1-3]. Clearly, it is important to understand the underlying mechanisms of deformation in gold at limited length scale. Molecular dynamics (MD) simulation has been commonly used to investigate the atomic-level mechanisms of plastic deformation at high strain rate in gold nanobeams and nanowires [4-10]. In recent MD work, Afanasyev and Sansoz [10] have studied the compression behavior of gold nanopillars (12 nm in diameter) consisting of nanoscale twin boundaries, a special type of grain boundary existing in this material. It was found that the presence of twin boundaries strongly influences the strength of gold nanopillars. Strengthening effects by interfacial plasticity were also found to largely depend on the twin interspacing. However, meaningful results related to the strength of gold nanopillars deformed by nanoindentation can only be accomplished if the influences of microstructure and sample size are fully understood. Particularly, further research effort must be undertaken to describe the bulk behavior of nano-twinned gold under uniaxial compression.

In this work, we used MD simulations to investigate the atomic mechanisms of plasticity in bulk nano-twinned gold under compression. A 3D, fully periodic simulation box was used to represent the bulk behavior of gold, excluding the effects of free surfaces. The deformation of single crystal Au was also considered. The next section describes the simulation method. The last section presents the effects of twin boundary on the compression behavior, and the atomic mechanisms operative at the intersection between slip and twin boundaries in bulk gold.

SIMULATION METHOD

Classical MD simulation was performed using LAMMPS Molecular Dynamics Simulator [11]. The interatomic potential used was an embedded-atom-method potential for FCC gold developed by Grochola et al. [12]. This potential was found to better predict the stacking fault and surface energies obtained experimentally, as opposed to other potentials in literature. The geometry of the model was a 200Å-wide cube with periodic boundaries in all three directions. The geometry and crystal orientations are shown in Figure 1. A typical model included about 0.5 million atoms. The simulations were performed in constant NVT ensemble at 300 K using a Nose/Hoover thermostat. The time step and entire simulation run were 5 fs and 2.5 ns, respectively. The model was first relaxed for 3000 steps (15 ps) to zero pressures along all three axial directions. Compression was performed on the relaxed structure by uniaxially shrinking the box at constant engineering strain rate (4×10^{7} s^{-1}) while keeping the volume constant by proportionally expanding the box along the lateral directions. The loading direction was the [111] direction, normal to the plane of the twins (Figure 1). The compression stress was averaged both spatially over the total volume and temporally for 1000 steps (5 ps). The yield strength was calculated from the equivalent von-Mises stress at yielding, which takes into account the stress triaxiality along the three directions of space [13]. We simulated the deformation of 1 single crystal and 8 twinned structures whose twin interspacing varied from 2 nm to 16 nm.

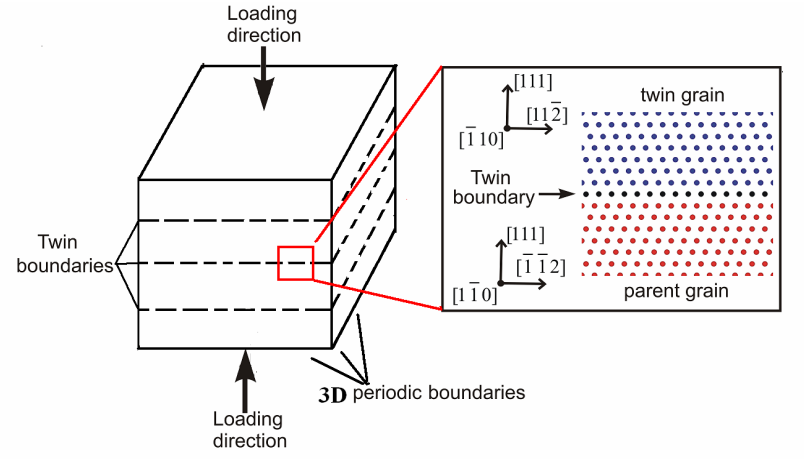

Figure 1. Atomic representation of bulk gold with three pre-existing growth twin boundaries. Close up view on the atomic structure and orientation at a twin boundary.

RESULTS AND DISCUSSION

Bulk compression behavior of single crystal and nano-twinned gold

Figure 2a represents the simulated stress-strain curves for single crystal and nano-twinned gold under uniaxial compression. This figure shows that the peak stress value

corresponding to the limit of elasticity increased as the twin interspacing was decreased. It should be noticed that the yield strength values of all bulk samples (> 8 GPa) were found to be significantly higher than the strength of 12 nm-diameter gold nanopillars (< 6 GPa) reported elsewhere [10]. This difference can be attributed to the fact that the bulk behavior was simulated from a defect-free model while, in nanopillars, free surfaces play an important role as sources of dislocations, thus decreasing the yield stress. Furthermore, Figure 2b represents the variation of yield strength as a function of the twin interspacing. This figure shows a small, non-monotonic increase in yield strength as the twin interspacing is decreased. The yield strength values are equal to 8.15 GPa and 8.5 GPa for a twin interspacing of 16 nm and 2 nm, respectively, which corresponds to a 0.35 GPa increase in yield stress. By comparison, the increase in yield strength was found to be twofold larger in 12 nm-diameter gold nanopillars for the same twin interspacings [10]. It is also worth noting in Figure 2 that the yield strength of the single crystal model is equal to 8.21 GPa. Therefore, the yield strength did not drastically change between bulk single crystal and twinned gold. We can therefore conclude from our simulations that strengthening effects related to the twin size are less significant in bulk gold than in 12 nm-diameter gold nanopillars. This conclusion also supports the idea that the underlying mechanisms of interfacial plasticity at twin boundaries may be influenced by the sample size, resulting in differences between bulk and nanopillar geometries, as shown below.

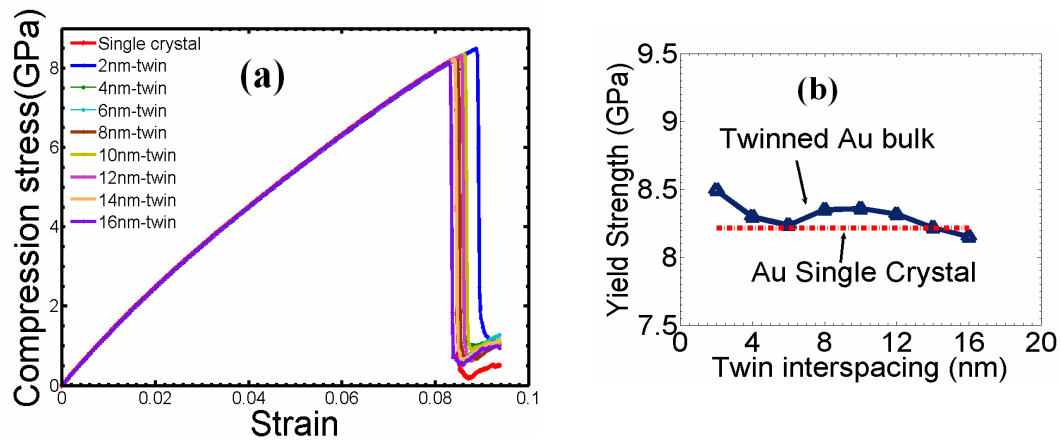

Figure 2. Bulk compression behavior of single crystal and nano-twinned gold by MD simulation. (a) Stress-strain curves. (b) Yield strength vs. twin interspacing in bulk gold.

Atomic mechanisms at the intersection between dislocation and twin boundary

Figure 3 shows the atomic structures of bulk gold with 8 nm-interspaced twin boundaries before and after a compression strain of ~ 9%. Intersection of slip dislocations with the twin boundaries was found to account for the differences in yielding phenomena. More specifically, in Fig. 3b corresponding to the plastically-deformed structure, it can be seen that a large number of stacking faults from the crystal lattice (highlighted by dark blue-colored atoms) exists at the

intersection with twin boundaries. In this figure, it is also important to note the formation of <111> atomic steps on the twin planes. Such steps clearly show the occurrence of interfacial plasticity at the twin boundaries in simulated bulk gold.

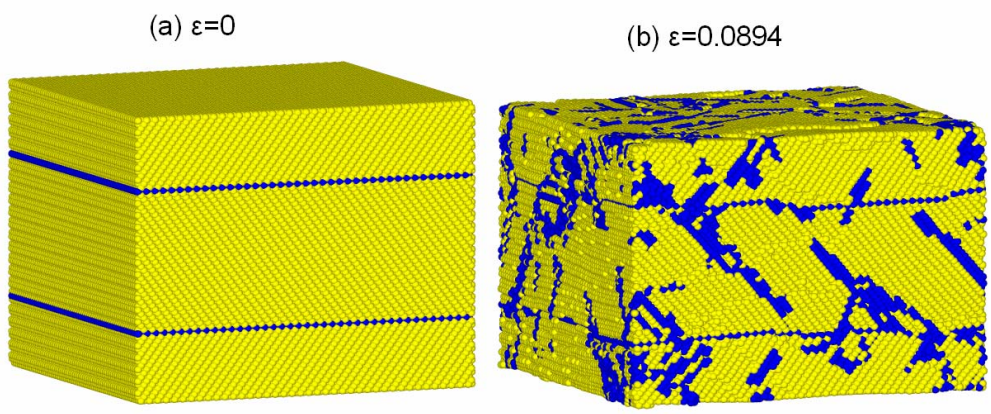

Figure 3. Atomistic model of bulk gold with 8 nm-interspaced twin boundaries under uniaxial compression. (a) Initial geometry before compression. (b) Structure with stacking faults and dislocations after yielding. Atoms are colored based on their centrosymmetry. Atoms in dark blue color represent stacking faults.

Atomistic details of the intersection between dislocations and twin boundaries at the onset of yielding are presented in Figure 4. In this figure, the twin interspacing corresponds to 8 nm. Figure 4a shows that the onset of plasticity is related to the activation of a $(11\bar{1})\langle 011\rangle$ slip in the grain separated by two twin boundaries. At this stage, each perfect <011> dislocation is dissociated into two <112> Shockley partial dislocations (a leading partial dislocation and a trailing partial dislocation). In Figure 4b, the leading partial is found to interact with the twin boundaries. It is shown in Figure 4c that the partial dislocations are directly transmitted across the upper and lower twin boundaries to form perfect (001)<110> dislocations in the twin grains. During this process, atomic steps corresponding to the formation of 1/3 [111] sessile Frank dislocations are left on the twin boundaries.

The atomic mechanism described above is different from the mechanisms of interfacial plasticity found in gold nanopillars under compression [10]. In the latter case, the mechanisms were related to the absorption and desorption [14] of both leading and trailing partials and the formation of Lomer-Cottrell locks and glissile twin dislocations that moved in the (111) plane of the twin boundary. A major difference is that glissile twin dislocations were not observed in the present study on bulk gold. Instead, the twin-slip reactions resulted in the formation of sessile Frank dislocations, which remained fixed on the twin boundary. This mechanism is in good agreement with experimental observations on bulk nano-twinned copper [15]. However, caution should be exercised here in comparing the different deformation modes at twin boundaries between bulk and nanopillar geometries, because the stress triaxiality in the bulk model may also play a role on the mechanisms.

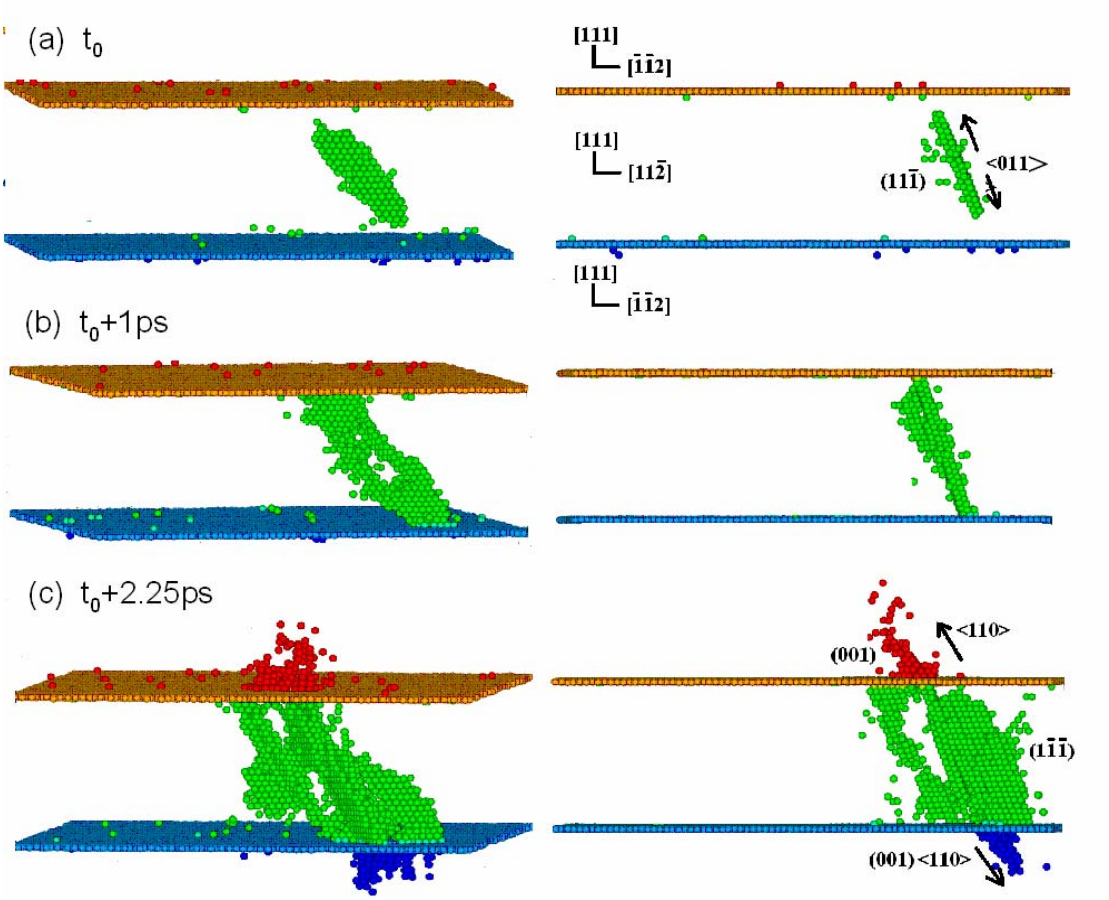

Figure 4. Atomistic details of the intersection between slip dislocations and twin boundaries in bulk nano-twinned gold. Atoms are colored based on their position with respect to the twin planes. Atoms in light blue and gold are present in the initial twin boundaries. Green-colored atoms between the two twin boundaries represent the slip dislocation. Atoms in red and blue colors belong to the transmitted dislocations. t_0 represents the time at the onset of yielding.

CONCLUSIONS

MD simulations have been carried out to characterize the slip behavior and plastic deformation of bulk nano-twinned gold at 300 K under uniaxial compression. We found in bulk nano-twinned gold simulated with 3D periodic boundary condition, that the limit of elasticity increased as the twin interspacing was decreased. However, strengthening effects related to the twin size were found to be less significant in bulk gold than in 12 nm-diameter gold nanopillars [10]. Our conclusions also suggested that the underlying mechanisms of interfacial plasticity at the intersection of dislocations with twin boundaries were different between bulk and nanopillar geometries. In the latter case, the reaction mechanisms at twin/slip intersection were related to the formation of Lomer-Cottrell locks and glissile twin dislocations that moved in the (111) plane of the twin boundary while, on bulk gold, the twin-slip reactions resulted in the formation of

sessile Frank dislocations, which remained fixed on the twin boundary. This study showed that it is critically important to consider the sample size in the plasticity of metal nanopillars with nanoscale growth twins. This computational work may also help us interpret the results of nanoindentation experiments on compressed nanosized pillars.

ACKNOWLEDGEMENTS

Support from the Vermont Advanced Computing Center under Phase II NASA grant # NNG 06GE87G is gratefully acknowledged.

REFERENCES

1. J. R. Greer, W. C. Oliver and W. D. Nix, *Acta Mater.* **53**, 1821 (2005).
2. J. R. Greer and W. D. Nix, *Phys. Rev. B* **73**, 245410 (2006).
3. C. A. Volkert and E. T. Lilleodden, *Phil. Mag.* **86**, 5567 (2006).
4. J. Diao, K. Gall and M. L. Dunn, *Nano Lett.* **4**, 1863 (2004).
5. J.-S. Lin, S.-P. Ju and W.-J. Lee, *Phys. Rev. B.* **72**, 085448 (2005).
6. B. Hyde, H. D. Espinosa and D. Farkas, *JOM* September, 62 (2005).
7. J. Diao, K. Gall, M. L. Dunn and J. A. Zimmerman, *Acta Mater.* **54**, 643 (2006).
8. E. Rabkin and D. J. Srolovitz, *Nano Lett.* **7**, 101 (2007).
9. E. Rabkin, H.-S. Nam and D. J. Srolovitz, *Acta Mater.* **55**, 2085 (2007).
10. K. A. Afanasyev and F. Sansoz, *Nano Lett.* **7**, 2056 (2007).
11. S. J. Plimpton, *J. Comp. Phys.* **117**, 1 (1995); http://lammps.sandia.gov/
12. G. Grochola, S. P. Russo and I. K. Snook, *J. Chem. Phys.* **123**, 204719 (2005).
13. W. F. Hosford. *Mechanical Behavior of Materials*, Cambridge University Press (2005)
14. T. Zhu, J. Li, A. Samanta, H. G. Kim and S. Suresh, *Proc. Natl. Acad. Sci. U. S. A.* **104**, 3031 (2007).
15. L. Lu, Y. Shen, X. Chen, L. Qian and K. Lu, *Science* **304**, 422 (2004).